Quaternary Science Reviews 33 (2012) 87–99

Contents lists available at SciVerse ScienceDirect

Quaternary Science Reviews

journal homepage: www.elsevier.com/locate/quascirev

Was the 12.1 ka Icelandic Vedde Ash one of a kind?

C.S. Lane [a,*], S.P.E. Blockley [b], J. Mangerud [c,d], V.C. Smith [a], Ø.S. Lohne [c,d], E.L. Tomlinson [e], I.P. Matthews [b], A.F. Lotter [f]

[a] Research Laboratory for Archaeology and the History of Art, University of Oxford, Dyson Perrins, South Parks Road, Oxford OX1 3QY, UK
[b] Centre for Quaternary Research, Department of Geography, Royal Holloway University of London, UK
[c] Department of Earth Science, University of Bergen, Norway
[d] Bjerknes Centre for Climate Research, Bergen, Norway
[e] Department of Earth Sciences, Royal Holloway University of London, UK
[f] Institute of Environmental Biology, Palaeoecology, Laboratory of Palaeobotany and Palynology, University of Utrecht, The Netherlands

ARTICLE INFO

Article history:
Received 20 June 2011
Received in revised form
22 September 2011
Accepted 11 November 2011
Available online 14 December 2011

Keywords:
Vedde Ash
Katla
Younger Dryas
Tephrochronology
Cryptotephra

ABSTRACT

The Vedde Ash is the most important volcanic event marker layer for the correlation of Late Quaternary palaeoenvironmental archives in Europe and the North Atlantic. First defined from its type site localities near Ålesund, Western Norway, the Vedde Ash has now been traced across much of northern and central Europe, into northwest Russia, within North Atlantic marine sediments and into the Greenland ice cores. The Vedde Ash is thought to derive from an eruption of the Katla volcano in Iceland that occurred midway through the Younger Dryas/Greenland Stadial 1 (GS-1), ~12.1 ka BP. Visible and cryptotephra deposits of the Vedde Ash have been found in numerous stratified sites with robust chronologies, which allow its age to be constrained and its dispersal to be mapped. The eruption must have been highly explosive, however few proximal outcrops have been confirmed and this crucial ash layer remains almost exclusively distally-described and characterised using major element glass compositions. The widespread distribution, stratigraphic associations and consistent major element glass chemistry have led the Quaternary tephrochronological community to see the Vedde Ash as a robust and unique chronological marker layer for the Last Glacial to Interglacial Transition (~10–18 ka BP). Here we present new glass analyses of the Vedde Ash from multiple sites around the dispersal area, using a full suite of compositional analysis, including for the first time, single-grain trace element data. These data demonstrate the strong compositional coherence of Vedde Ash deposits. However, comparison with major, minor, and trace element compositional data from several other distally-described Icelandic tephras reveals that both before and after the Younger Dryas chronozone, there were eruptions that generated widespread tephra layers that have comparable glass shard compositions to the Vedde Ash. This implies that these numerous events not only hail from the same volcanic system, but that the melts share similar crystallisation trends and mixing patterns prior to eruption. It seems therefore that composition alone is insufficient for the correlation of some widespread tephra layers: good stratigraphic information and/or robust dating control are also essential.

1. Introduction

1.1. The most widespread Icelandic event horizon

The Icelandic Vedde Ash (VA) was first detected by Mangerud et al. (1984) within lake sediments of the Ålesund and Nordfjord regions of western Norway. Here it is preserved as a visible layer (0–50 cm thick, e.g. Koren et al., 2008) deposited midway through the Younger Dryas Stadial chronozone (Mangerud et al., 1974), an abrupt cold event during the Last Glacial to Interglacial Transition (LGIT). In the widely used INTIMATE event stratigraphy (Lowe et al., 2008), the YD is broadly equivalent to Greenland Stadial 1 (GS-1). Since then, the VA has been reported in over 50 sites outside the Younger Dryas ice sheet margin in western and northern Norway (e.g. Johansen et al., 1985; Svendsen and Mangerud, 1990; Bondevik et al., 1999; Sønstegaard et al., 1999; Lohne et al., 2007; Vorren et al., 2009) and over 30 sites stretching across the rest of Europe, from Greenland to NW Russia and as far south as Italy (e.g. Wastegård et al., 2000a; Mortensen et al., 2005; Lane et al., in press-a), as both visible and non-visible (crypto-) tephra layers (Fig. 1). The

* Corresponding author. Tel.: +44 1865 285203; fax: +44 1865 285220.
E-mail address: Christine.lane@rlaha.ox.ac.uk (C.S. Lane).

0277-3791/$ – see front matter © 2011 Elsevier Ltd. All rights reserved.
doi:10.1016/j.quascirev.2011.11.011

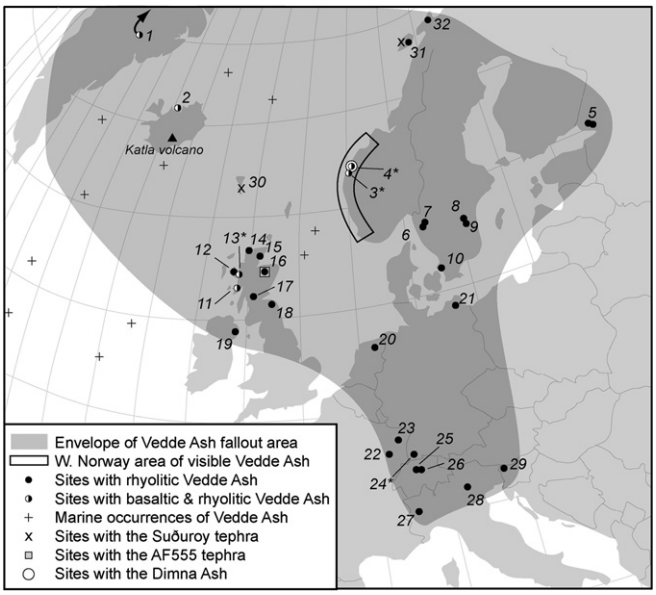

Fig. 1. Map showing locations where the Vedde Ash (VA), Suðuroy tephra, Dimna Ash and AF555 tephra have been identified as primary airfall layers in stratified terrestrial sites. Sites sampled for this study are marked with *. Grey shaded area demarks the currently known extent of fallout deposits of the VA, not taking into account likely ice-rafted marine sediment layers. Black outline box highlights the areas of western Norway that contain the VA as a visible layer (Fægri, 1940; Mangerud et al., 1984; Johansen et al., 1985; Svendsen and Mangerud, 1990; Bondevik et al., 1999; Sønstegaard et al., 1999; Bondevik and Mangerud, 2002; Lohne et al., 2004, 2007, in press; Knudsen, 2006; Lohne, 2006; Koren et al., 2008; Krüger et al., 2011). Numbered sites as followings: 1. NGRIP (Mortensen et al., 2005); 2. Lake Torfadalsvatn (Björck et al., 1992); 3. Kråkenes (Mangerud et al., 1984); 4. Dimnamyra (Koren et al., 2008); 5. Karelian Isthmus (Wastegård et al., 2000a); 6. Lake Madtjärn (Wastegård et al., 1998); 7. Lake Götejön (Schoning et al., 2001); 8. Fågelmossen (Björck and Wastegård, 1999); 9. Högstorpsmossen (Björck and Wastegård, 1999); 10. Lake Kullatorpssjön (Wastegård et al., 2000b); 11. Loch an t'Suidhe (Lowe, 2001; Mackie et al., 2002); 12. Druim Loch (Pyne-O'Donnell, 2007); 13. Loch Ashik (Davies et al., 2001); 14. Lochan An Druim (Ranner et al., 2005) 15. Borrobol (Turney et al., 1997); 16. Abernethy Forest (Matthews et al., 2011); 17. Tynaspirit West (Turney et al., 1997); 18. Whitrig Bog (Turney et al., 1997); 19. Roddans Port (Turney et al., 2006); 20. Kostverloren Veen (Davies et al., 2005); 21. Endinger Bruch (Lane et al., in press-b); 22. Marais de la Maxe (Walter-Simonnet et al., 2008); 23. Lac de Sewen (Walter-Simonnet et al., 2008); 24. Rotmeer (Blockley et al., 2007); 25. Soppensee (Blockley et al., 2007); 26. Rotsee (Lane et al., in press-a); 27. Lago Piccolo di Avigliana (Lane et al., in press-a); 28. Lavarone (Lane et al., in press-a); 29. Lake Bled (Lane et al., 2011a); 30. Hovsdalur (Wastegård, 2002); 31. Vestvågøy (Pilcher et al., 2005); 32. Lake Æråsvatn (Vorren et al., 2009). A number of marine core locations where the VA (or North Atlantic Ash Zone 1) has been reported are also shown (Long and Morton, 1987; Kvamme et al., 1989; Sejrup, 1989; Bard et al., 1994; Haflidason et al., 2000; Thornalley et al., 2011).

ice-rafted North Atlantic Ash Zone 1 has been correlated to the VA, but the layer also contains several other ashes (Mangerud et al., 1984; Kvamme et al., 1989; Lacasse et al., 1995).

The widespread tephra layers correlated to the VA are consistently found within sediments and biozones associated with the Younger Dryas Stadial (Fig. 2), providing stratigraphic evidence in support of the chemical correlation. Radiocarbon age estimates of sediments surrounding the VA in Norway and Sweden are 11 844–12 388 cal a BP and 11 833–12 511 cal a BP, respectively (Birks et al., 1996; Wastegård et al., 1998; calibrated using IntCal09, Reimer et al., 2009). These ages are in good agreement with the more precise age of 12 007–12 235 GICC05 a BP established from annual layer counting in Greenland ice cores (Rasmussen et al., 2006). Recognition of the VA in palaeoenvironmental records therefore supplies an isochronous marker horizon with an independently derived calendrical age estimate, which can therefore be used to constrain or test age-models. Used in this way, the VA provides a means to correlate palaeoenvironmental records across a network of sites in Europe and the North Atlantic, within which the potential exists to test the timing of environmental responses to palaeoclimatic change across continental distances (e.g.: Lowe, 2001; Lowe et al., 2008; Lane et al., 2011a).

More recently, the VA has been used as a critical marker horizon delimiting the earlier and later parts of the Younger Dryas (Lowe, 2001; Bakke et al., 2009; Lane et al., in press-a). The Early Younger Dryas in northern Europe is thought to be characterised by cold and stable conditions, however immediately after the deposition of the VA these stable conditions are thought to change with oscillating cold and warm temperatures brought about by intrusions of warm water into the North Atlantic changing the position of westerly winds (Bakke et al., 2009).

The VA is typical of many Late Quaternary Icelandic tephra layers that have been found within sediment sequences of the North Atlantic and Europe, in that it has been recognised almost exclusively in distal settings. This is because the prevailing glacial conditions on Iceland have erased and eroded most proximal tephra deposits and the soils that could have contained them (Haflidason et al., 2000; Ingólfsson et al., 2009). Correlations have also been suggested between the VA and outcrops on Iceland of the Skógar Tephra, which shares the full chemical range observed in the VA (Norddahl and Haflidason, 1992), and the Sólheimar Ignimbrite, which lacks a basaltic phase (Lacasse et al., 1995). However, these terrestrial deposits lack unequivocal stratigraphic context and independent dating to confirm their Younger Dryas age, thus these correlations remain controversial (c.f. Van Vliet-Lanoë et al., 2007; Ingólfsson et al., 2009; Tomlinson et al., submitted for publication).

1.2. Research agenda

After the discovery and geochemical characterisation of the VA (Mangerud et al., 1984) and the Early Holocene Saksunarvatn Tephra (Mangerud et al., 1986), the applications of tephrostratigraphy and tephrochronology rapidly increased. Of particular importance were the developments in cryptotephra methods, which now allow correlation of even the most far-travelled, non-visible, tephra deposits (Turney et al., 1997; Blockley et al., 2005). As more far-travelled tephras are discovered however, some tephra layers are being detected that have very similar major element glass compositions, which indicates that similar magma compositions were generated from separate eruptions over 1000s of years (e.g., Larsen et al., 2001; Davies et al., 2004; Koren et al., 2008; Brendryen et al., 2010). Thus major and minor element compositions alone may not be sufficient to confidently correlate all distal tephra deposits. These findings have significant implications for distal tephrochronology and highlight the importance of making careful and secure correlations between tephra horizons. This is especially important when working with small compositional datasets from low concentration samples that may not represent an eruption's full chemical range due, for example, to changes in the wind direction during the eruption.

To date, the correlation of most occurrences of the VA has been based upon the major and minor element composition of the glass shards, coupled with secure stratigraphical and chronological evidence. Distal deposits of the VA are mostly comprised of rhyolitic shards but in some sites, particularly those around the North Atlantic rim, basalt and/or intermediate components are present (Figs. 1 and 3). However, the true spatial distribution of the basaltic phase of the VA may be skewed by the floatation methods employed to extract tephra, which preference the lighter, rhyolitic fraction (Turney, 1998; Blockley et al., 2005).

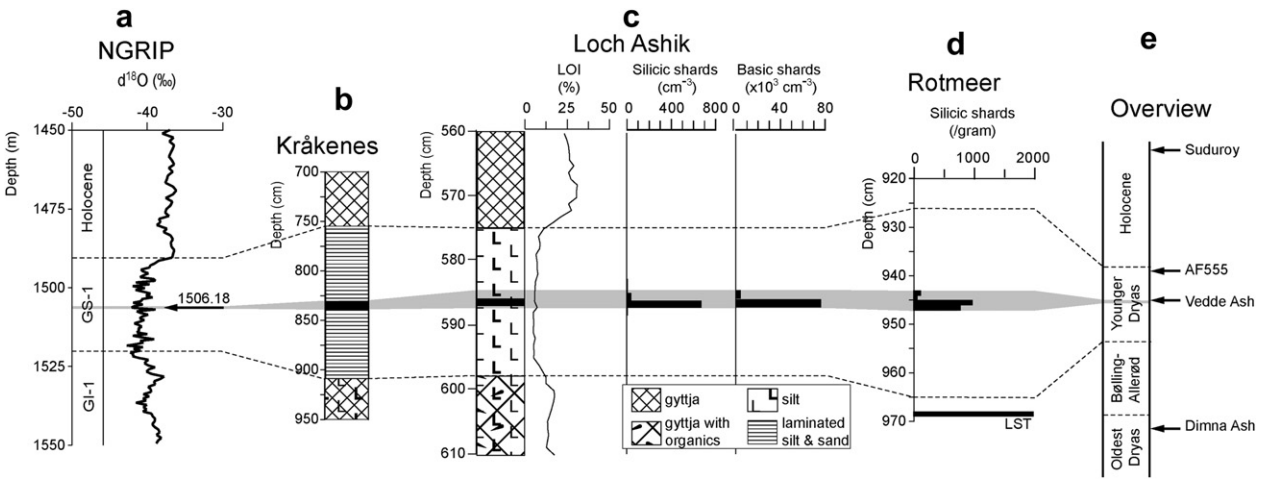

Fig. 2. The stratigraphic position of the Vedde Ash (VA). (a) In the NGRIP ice core the VA lies within Greenland Stadial 1 (GS-1) at 1506.18 metres depth (Mortensen et al., 2005; Rasmussen et al., 2006); (b) In Kråkenes, Norway, the VA is a visible layer midway through the Younger Dryas stadial sediments (Mangerud et al., 1984; Birks et al., 2000); (c) In Loch Ashik, Scotland, both rhyolitic and basaltic shards are found within silts associated with the Loch Lomond stadial (British Isles equivalent to the Younger Dryas), as confirmed by the loss-on-ignition (LOI) profile (this study; Davies et al., 2001; Pyne-O'Donnell, 2011); (d) in Rotmeer, Switzerland, only rhyolitic shards have been found as a cryptotephra layer (Blockley et al., 2007; Lane et al., in press-a). This layer lies approximately 25 cm above the Laacher See Tephra (LST). (e) Overview stratigraphical profile (not to scale) showing the position of the VA in relation to the chemically similar tephra layers discussed in this paper: the Suðuroy tephra (Wastegård, 2002); the AF555 tephra (Matthews et al., 2011); the Dimna Ash (Koren et al., 2008).

Three far travelled cryptotephra layers have been defined from published terrestrial sites that have glass major element compositions very similar to the most far-travelled rhyolitic fraction of the VA (Figs. 3 and 4). These are the ~8 ka BP Suðuroy tephra, the 11.2–11.8 a BP AF555 tephra and the >15 ka BP Dimna Ash. The Suðuroy tephra was first described in a Holocene peat core from the Faroe Islands by Wastegård (2002). The age of the Suðuroy tephra is constrained by multiple radiocarbon dates and the identification of other Icelandic tephra horizons in the same sequence. The Suðuroy tephra lies ~140 cm above the Saksunarvatn tephra, which is dated in the NGRIP ice core to 10 208–10 386 GICC05 a BP (Rasmussen et al., 2006). The Suðuroy tephra has also been identified, in the same stratigraphic position in North Norway by Pilcher et al. (2005), confirming that it is a far-travelled Early Holocene-aged event horizon. The AF555 tephra was recently described by Matthews et al. (2011) from late Younger Dryas sediments of an infilled channel sequence in Abernethy Forest, Scotland. In the Abernethy Forest sequence the AF555 tephra lies ~40 cm above a mid Younger Dryas tephra, which is correlated to the VA. No tephra shards are present in between these two layers, suggesting that they are two separate eruptive events (see Matthews et al., 2011). The Dimna Ash was found in the Dimnamyra lacustrine sediment sequence from Western Norway by Koren et al. (2008) (Fig. 1). This sequence has multiple radiocarbon dates, which provide a minimum age for the Dimna Ash of 15 100 cal a BP, ~3000 years older than the VA. The tephra lies within lagoonal silts and sands believed to have been rapidly deposited during the last deglaciation. The Dimna Ash lies stratigraphically *below* the VA in Dimnamyra (Koren et al., 2008).

Within the marine realm, pre-Younger Dryas tephra deposits with glass compositions comparable to the Vedde Ash have been described by Bond et al. (2001) and more recently, Thornalley et al. (2011). The latter have reported the frequent occurrence of rhyolitic tephra shards that are compositionally similar to the VA in marine core sediments from the South Iceland Rise, up to 3000 years earlier than the Vedde Ash, which is present higher up in the stratigraphy of the same core. These tephra shards appear to be of equivalent or greater age to the Dimna Ash of Koren et al. (2008).

It seems therefore that a number of eruptions have occurred that have produced widely dispersed tephra that can, at present, only be differentiated from the far-travelled rhyolitic fraction of the VA on the basis of their stratigraphic position. Hence, the potential exists to incorrectly identify these layers in poorly stratified sites. Here we have attempted to address this problem by definitively characterising the VA from Kråkenes, one of the type sites in Norway (Mangerud et al., 1984). VA samples from other sites from around the dispersal area have also been characterised to the same level and compared to the Kråkenes dataset and other published examples, to test the reported widespread dispersal of this important marker horizon. The composition of the VA is then compared to that of the Suðuroy tephra, the AF555 tephra, the Dimna Ash and the R1 tephra layer to evaluate the discriminative potential of glass compositional data alone.

2. Methods

2.1. Sites and samples

The positions of all sites from which samples were used in this study are indicated on Fig. 1 with a superscript asterisk.

Primary data collection was carried out on samples of the VA from three previously published lake sites, spread out across the southern and eastern dispersal area of the VA tephra. These were: Kråkenes, western Norway (Mangerud et al., 1984; Birks et al., 2000), Loch Ashik, Scotland (Davies et al., 2001; Pyne-O'Donnell, 2011), and Rotmeer, southern Germany (Blockley et al., 2007). Within these sites the tephra layer correlated to the VA is located midway through the sediments associated with the Younger Dryas Stadial, providing good stratigraphical consistency (Fig. 2). The VA is visible in Kråkenes and samples were taken from core 502.46, previously published by Birks et al. (2000). The Loch Ashik sample was extracted from the visible VA layer in a core retrieved from the western edge of the loch, close to the location of the core sampled by Davies et al. (2001) and the 'site 1' sediment sequence published by Pyne-O'Donnell (2011). The VA layer was represented by a ca. 1 cm thick 'black band' between 586–587 cm depth, which comprises concentrations of 667 rhyolitic shards and ca. 76,000

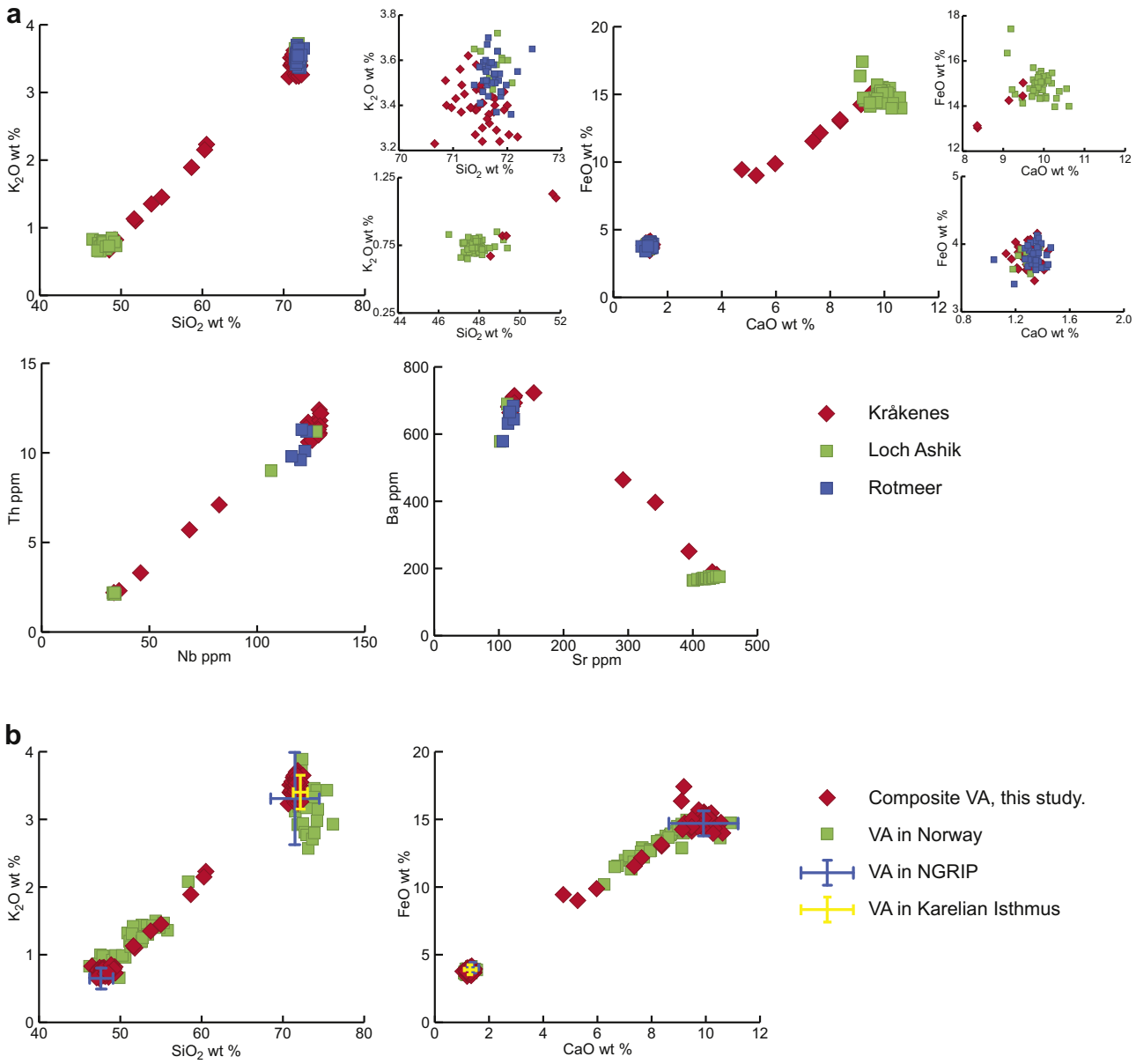

Fig. 3. Selected elemental bi-plots of Vedde Ash (VA) glass chemistry. All major and minor data plotted as normalised values. (a) Sites analysed within this study (Kråkenes, Loch Ashik and Rotmeer), with expanded plots for each of the end-members shown to clarify the major element diagrams. (b) Correlation of the VA data from this study with published compositional data for the VA. Norwegian VA data is compiled from sites reported in Mangerud et al. (1984) and Kvamme et al. (1989). The mean and 2σ range of the VA in NGRIP (Mortensen et al., 2005) and in the Karelian Isthmus, NW Russia (Wastegård et al., 2000a) are also shown (Colour images available online).

basaltic shards per cm^{-3} of sediment (Fig. 2). The only cryptotephra sampled in this study came from Rotmeer core RO6, where it is found in concentrations of ~1000 shards per gram of (dry) sediment (Blockley et al., 2007).

The published compositional ranges of the VA in western Norway (Mangerud et al., 1984; Kvamme et al., 1989) and in NGRIP (Mortensen et al., 2005) are included in this study, to assess compositional variability across the full distal dispersal area of the tephra. NGRIP is the most north-westerly known deposit of the Vedde Ash.

The Dimna Ash was also sampled from the Dimnamyra type site in western Norway, to assess whether it is compositionally distinct from the VA. Published major and minor element data for the Suðuroy tephra (Wastegård, 2002), the AF555 tephra (Matthews et al., 2011) and the R1 tephra shards are also compared to the VA and Dimna Ash data generated in this study.

2.2. Chemical characterisation

The chemical composition of all tephra samples was measured using single-grain micro-analysis of glass shards. No associated primary volcanic mineral fractions were identified with the distal VA deposits.

Major and minor elements were measured using wavelength-dispersive electron probe micro-analysis (WDS-EPMA) on the Jeol JXA8600 at the Research Laboratory for Archaeology and the History of Art, University of Oxford. An accelerating voltage of 15 keV, beam current of 6 nA and a defocused (10 μm) beam were used. Ten major and minor elements were analysed with the following on-peak count times: Na 10 s; Si, Al, K, Ca, Fe, Mg 30 s; Ti, Mn, 40 s; P 60 s. Secondary glass standards from the MPI-DING fused volcanic glass secondary standards collection (Atho-G and StHs6/80-G, Jochum et al., 2006) were used to monitor both

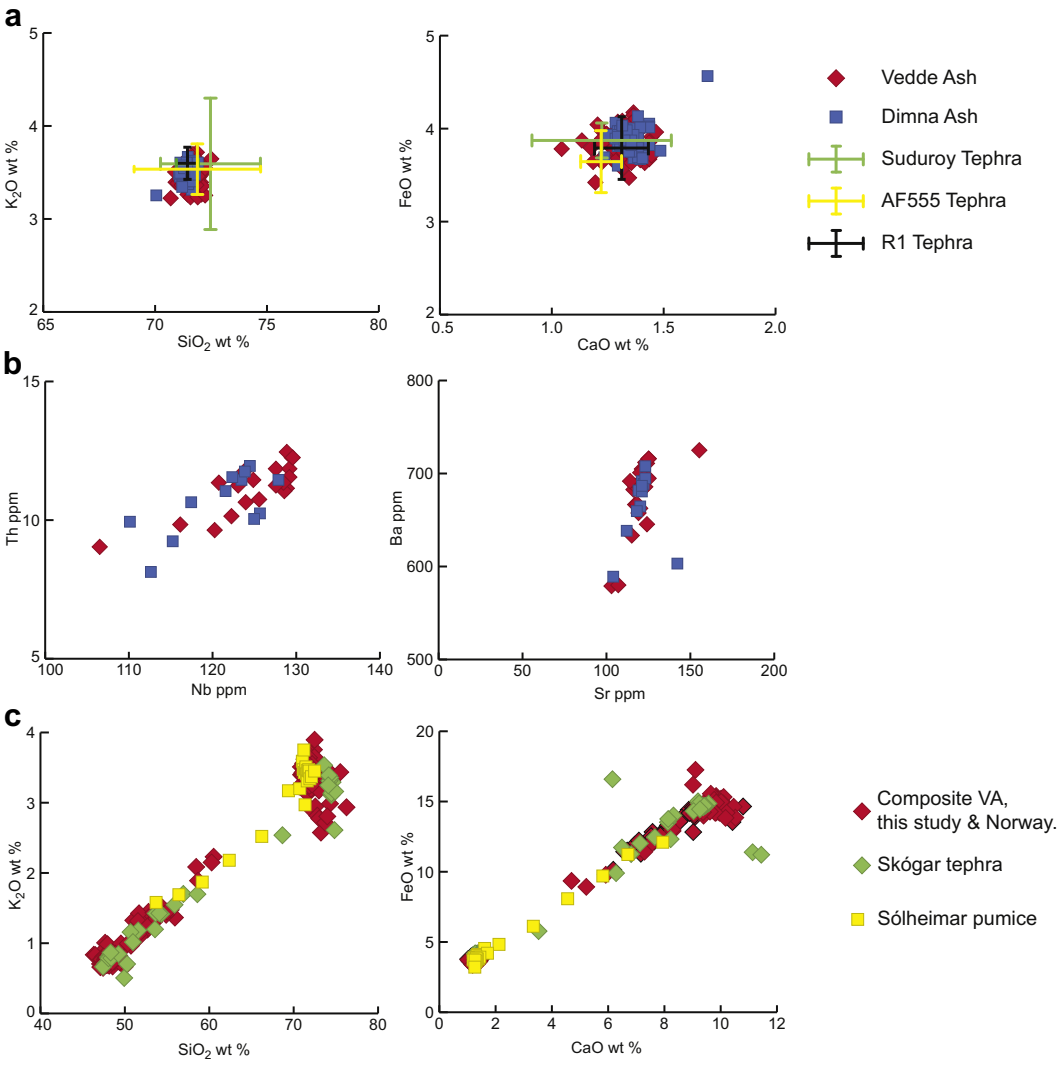

Fig. 4. Selected bi-plots comparing the composition of the Vedde Ash (VA), the Dimna Ash (Dimna Ash) and other chemically similar tephras. (a) Major element compositions, with 2σ ranges for the Suðuroy (Wastegård, 2002), AF555 (Matthews et al., 2011) and R1 (Thornalley et al., 2011) tephras. (b) Trace element compositions of the VA and Dimna Ash (see also Fig. 5). (c) Comparison of the composite VA data (from this study and the Norwegian records, as in Fig. 3b) with glass chemistry data from the Skógar tephra, in Northern Iceland (Norddahl and Haflidason, 1992) and pumice samples from the Sólheimar ignimbrite in Southern Iceland (Tomlinson et al., submitted for publication) (Colour images available online).

precision and accuracy of the microprobe analyses (Supporting Information Table 1). Major element (SiO_2, Al_2O_3, FeO, CaO, Na_2O, K_2O) precision on secondary standard analyses ranges from <1 to <10% (at 2σ), precision for the less abundant elements varies between 10–40%.

Trace element analysis was carried out by laser ablation inductively coupled plasma mass spectrometry (LA-ICP-MS), using an Agilent 7500 ICP-MS coupled to a 193 nm Resonetics ArF eximer laser ablation system, in the Department of Earth Sciences, Royal Holloway University of London (Müller et al., 2009). Analytical protocols and data quantification followed those described in Tomlinson et al. (2010). A 5 Hz repetition rate and 40 s sample and gas blank count times were used. NIST 612 was used as a standard for calibration, with ^{29}Si as the internal standard element having been previously measured by WDS-EPMA within each individual grain. Laser spot sizes of between 25 and 57 μm were used according to the size of the glass shards. For consistency with WDS-EPMA, the Atho-G and StHs6/80-G MPI-DING secondary glass standards were used to monitor precision and accuracy (Supporting Information Table 2). Precision (at 2σ) averages < 10% for Rb to Ce and 10–20% for Pr-U.

3. Results

3.1. The composition of the Vedde Ash

The results of WDS-EPMA and LA-ICP-MS are shown in Tables 1 and 2 and are summarised in elemental plots in Figs. 3–5. These results are consistent with previously published major and minor element glass compositions for the VA from the type localities in Norway and from other sites around the dispersal area (Fig. 3). These data also present the first single-grain trace element analysis of the VA and the Dimna Ash. The trace element data support the existing major element correlation of the tephras in Rotmeer and Loch Ashik to the VA in its type locality (Fig. 3).

The VA is characterised by two end-member glass compositions (mafic and silicic), which are represented in varying proportions within the study sites. The silicic member is a K-rich, Si-undersaturated rhyolite, which is found in all sites and characterised by (anhydrous) glass compositions of approximately 70.0–72.5 wt % SiO_2, 0.2–0.4 wt % TiO_2, 3.4–4.2 wt % FeO, 0.2–0.3 wt % MgO, 1.1–1.7 wt% CaO, 4.9–5.6 wt % Na_2O, 3.2–3.7 wt % K_2O, 73–89 ppm Rb, 750–940 ppm Zr and 110–130 ppm Nb. The mafic

Table 1
WDS-EPMA results for all Vedde Ash and Dimna Ash samples included in this study. Major element precision (SiO_2, Al_2O_3, FeO, CaO, Na_2O, K_2O) ranges from <1 to <10% (at 2σ), minor element precision varies between 10–40%. Associated secondary standard analyses files (S/std file) can be found in Supplementary Information Table 1.

SiO_2 wt %	TiO_2 wt %	Al_2O_3 wt %	FeO tot wt %	MnO wt %	MgO wt %	CaO wt %	Na_2O wt %	K_2O wt %	P_2O_5 wt %	Total wt %	S/std File
Kråkenes_VA											
48.38	4.58	13.38	14.98	0.24	4.95	9.46	2.53	0.67	0.47	99.62	a
48.66	4.31	13.09	14.30	0.22	4.86	9.39	2.89	0.81	0.43	98.96	a
49.00	4.58	13.25	14.16	0.18	4.74	9.07	3.09	0.81	0.41	99.29	a
49.87	3.57	12.98	12.55	0.17	4.07	8.06	3.46	1.06	0.44	96.23	a
51.15	4.01	13.36	13.02	0.19	4.16	8.28	3.36	1.12	0.42	99.07	a
51.75	3.38	13.20	11.71	0.22	3.53	7.34	3.42	1.30	0.39	96.23	a
54.32	3.14	13.66	11.40	0.18	3.48	7.27	3.47	1.44	0.35	98.70	a
58.50	2.65	13.48	9.85	0.14	2.84	5.95	4.04	1.88	0.27	99.60	a
60.08	2.22	13.80	8.94	0.14	2.54	5.23	3.77	2.21	0.24	99.19	a
60.13	2.86	13.35	9.42	0.17	2.36	4.73	4.22	2.14	0.26	99.64	a
68.09	0.31	13.61	3.80	0.14	0.23	1.32	5.01	3.38	0.02	95.92	a
68.84	0.31	13.49	3.59	0.18	0.17	1.26	4.89	3.28	0.06	96.07	a
68.89	0.31	13.47	3.81	0.09	0.20	1.18	4.82	3.34	0.00	96.11	a
69.00	0.31	13.46	4.05	0.15	0.17	1.32	5.33	3.31	0.05	97.14	a
69.02	0.27	13.46	3.71	0.14	0.20	1.20	4.69	3.30	0.00	95.99	a
69.10	0.34	13.57	3.53	0.19	0.17	1.18	5.07	3.36	0.06	96.56	a
69.24	0.31	13.69	3.70	0.06	0.22	1.22	5.12	3.29	0.04	96.87	a
69.30	0.27	13.75	3.67	0.12	0.21	1.22	4.95	3.29	0.07	96.86	a
69.36	0.28	13.48	3.51	0.12	0.20	1.18	5.07	3.18	0.02	96.40	a
69.59	0.24	13.38	3.58	0.14	0.25	1.24	4.89	3.27	0.01	96.59	a
69.67	0.25	13.65	3.73	0.11	0.19	1.26	5.08	3.22	0.03	97.20	a
69.81	0.24	13.42	3.78	0.17	0.19	1.24	5.21	3.39	0.00	97.45	a
69.82	0.24	13.70	3.60	0.13	0.20	1.27	5.48	3.38	0.04	97.87	a
69.93	0.36	14.02	3.87	0.06	0.20	1.23	5.24	3.34	0.07	98.32	a
70.00	0.30	13.35	3.85	0.09	0.19	1.29	5.22	3.33	0.03	97.66	a
70.10	0.25	13.92	3.61	0.08	0.18	1.28	4.99	3.51	0.02	97.95	a
70.22	0.29	13.56	3.54	0.18	0.19	1.25	5.10	3.30	0.07	97.71	a
70.32	0.33	14.10	4.01	0.13	0.19	1.27	5.01	3.39	0.04	98.79	a
70.47	0.40	14.29	3.89	0.16	0.23	1.44	5.46	3.22	0.03	99.58	a
70.53	0.28	13.76	3.98	0.08	0.19	1.19	5.14	3.59	0.03	98.77	a
70.75	0.28	13.64	3.68	0.16	0.18	1.38	5.41	3.35	0.06	98.88	a
70.77	0.31	13.81	3.88	0.17	0.18	1.24	5.37	3.47	0.04	99.23	a
70.91	0.31	13.54	3.66	0.12	0.18	1.38	5.28	3.33	0.06	98.77	a
70.96	0.31	14.04	3.61	0.11	0.18	1.41	5.38	3.55	0.03	99.59	a
71.01	0.25	13.66	3.77	0.13	0.20	1.34	5.00	3.40	0.03	98.81	a
71.03	0.34	13.86	3.76	0.17	0.21	1.30	4.98	3.29	0.01	98.94	a
71.08	0.28	13.88	3.93	0.12	0.17	1.31	5.19	3.37	0.00	99.33	a
71.08	0.28	13.77	3.57	0.14	0.20	1.27	4.86	3.35	0.03	98.54	a
71.11	0.35	13.67	3.79	0.19	0.18	1.32	5.10	3.31	0.06	99.09	a
71.26	0.27	14.28	3.87	0.14	0.19	1.29	5.27	3.38	0.02	99.97	a
71.34	0.36	13.83	3.87	0.19	0.22	1.33	5.30	3.26	0.01	99.72	a
71.46	0.26	13.90	4.07	0.13	0.16	1.31	5.12	3.24	0.10	99.73	a
71.49	0.30	14.07	3.96	0.18	0.17	1.32	5.13	3.40	0.04	100.05	a
71.49	0.25	13.84	3.68	0.13	0.15	1.36	5.49	3.40	0.03	99.82	a
71.59	0.36	13.76	3.44	0.11	0.18	1.33	5.11	3.44	0.02	99.35	a
71.61	0.32	13.75	3.66	0.15	0.20	1.32	5.36	3.50	0.05	99.91	a
71.75	0.34	13.77	3.84	0.12	0.19	1.13	5.01	3.26	0.06	99.46	a
71.81	0.27	13.70	3.90	0.16	0.20	1.25	5.18	3.41	0.03	99.90	a
71.85	0.24	13.88	3.88	0.11	0.19	1.22	5.09	3.24	0.08	99.79	a
72.26	0.23	13.70	3.79	0.09	0.20	1.17	5.15	3.27	0.01	99.87	a
Loch Ashik_VA											
45.89	4.59	12.56	14.74	0.20	5.05	9.58	2.98	0.71	0.48	96.77	b
45.89	5.29	12.86	17.19	0.21	4.49	9.07	2.39	0.82	0.49	98.69	b
45.90	4.51	12.30	14.22	0.15	5.18	9.40	3.15	0.72	0.54	96.06	b
45.91	4.66	12.56	14.79	0.24	5.13	9.56	2.84	0.68	0.47	96.83	b
45.93	4.35	12.45	14.56	0.19	5.07	9.64	2.92	0.71	0.53	96.35	b
45.96	4.53	12.34	14.81	0.27	5.15	9.61	3.06	0.75	0.54	97.02	b
45.97	4.69	12.56	14.50	0.23	5.16	9.66	2.55	0.75	0.56	96.63	b
45.99	4.55	12.42	14.64	0.21	5.25	9.56	3.17	0.68	0.51	96.97	b
46.00	4.41	12.46	14.87	0.28	5.09	9.55	2.78	0.69	0.49	96.64	b
46.11	4.53	12.47	13.86	0.24	5.03	9.66	3.00	0.73	0.48	96.11	b
46.16	4.62	12.48	15.18	0.14	5.11	9.70	3.07	0.68	0.54	97.69	b
46.20	4.50	12.69	14.67	0.26	5.08	9.68	2.98	0.73	0.49	97.26	b
46.23	4.38	12.36	13.74	0.24	5.13	9.63	2.90	0.68	0.51	95.80	b
46.23	4.57	12.63	15.11	0.15	5.24	9.72	3.04	0.75	0.48	97.93	b
46.25	4.63	12.54	14.58	0.23	5.20	9.65	3.02	0.79	0.55	97.45	b
46.34	4.58	12.56	14.49	0.21	5.10	9.51	2.80	0.67	0.52	96.79	b
46.41	4.60	12.48	14.73	0.16	5.18	9.59	2.88	0.67	0.50	97.21	b
46.42	4.59	12.49	14.51	0.24	5.02	9.58	2.83	0.70	0.49	96.88	b
46.49	4.57	12.47	15.03	0.28	5.24	9.90	2.69	0.72	0.52	97.91	b
46.50	4.71	12.53	15.24	0.19	5.36	10.05	2.72	0.76	0.50	98.56	b
46.51	4.68	12.32	14.42	0.27	5.44	10.22	3.31	0.75	0.50	98.42	b

Table 1 (*continued*)

SiO_2 wt %	TiO_2 wt %	Al_2O_3 wt %	FeO tot wt %	MnO wt %	MgO wt %	CaO wt %	Na_2O wt %	K_2O wt %	P_2O_5 wt %	Total wt %	S/std File
46.53	4.54	12.43	14.21	0.24	5.01	9.64	2.74	0.76	0.54	96.64	b
46.54	4.57	12.35	14.79	0.27	5.03	9.49	3.07	0.76	0.62	97.49	b
46.61	4.62	12.42	14.96	0.19	5.23	9.77	2.74	0.70	0.54	97.78	b
46.63	4.74	12.45	14.37	0.25	5.28	9.58	3.21	0.76	0.57	97.84	b
46.65	4.49	12.54	14.28	0.24	4.98	9.32	2.87	0.71	0.52	96.58	b
46.70	4.54	12.30	13.96	0.25	4.84	9.38	2.53	0.71	0.56	95.77	b
46.73	4.52	12.62	14.81	0.15	4.96	9.61	2.55	0.73	0.51	97.19	b
46.76	4.47	12.87	14.52	0.20	5.08	9.55	2.92	0.78	0.49	97.64	b
46.76	4.62	12.61	14.67	0.19	5.04	9.57	3.03	0.74	0.51	97.73	b
46.76	4.56	12.70	15.46	0.27	4.87	9.58	3.00	0.69	0.54	98.44	b
46.76	4.68	11.70	13.76	0.21	4.64	8.80	2.81	0.69	0.64	94.70	b
46.79	4.53	12.76	13.97	0.13	5.15	9.66	2.96	0.72	0.54	97.22	b
46.87	4.51	12.67	14.67	0.27	4.87	9.55	2.93	0.79	0.54	97.67	b
46.88	4.53	12.78	14.49	0.20	5.01	9.63	2.88	0.68	0.62	97.71	b
46.89	4.90	12.69	16.06	0.25	4.54	8.94	2.62	0.78	0.56	98.23	b
46.93	4.55	12.55	14.87	0.19	5.08	9.66	2.60	0.71	0.53	97.67	b
46.95	4.58	12.74	14.75	0.22	4.85	9.62	2.86	0.76	0.50	97.84	b
46.97	4.63	12.49	15.00	0.24	5.06	9.68	3.00	0.71	0.48	98.27	b
47.03	4.66	12.85	14.89	0.26	5.32	10.10	2.85	0.71	0.49	99.15	b
47.05	4.44	12.24	14.50	0.24	5.44	10.37	2.56	0.76	0.59	98.19	b
47.07	4.60	12.73	14.88	0.21	5.09	9.96	2.61	0.79	0.51	98.44	b
47.12	4.62	12.75	14.90	0.31	4.99	9.82	3.07	0.72	0.57	98.88	b
47.14	4.47	12.68	13.70	0.24	5.63	10.40	2.52	0.66	0.47	97.92	b
47.19	4.58	13.34	14.27	0.20	5.16	10.27	3.38	0.65	0.49	99.52	b
47.20	4.45	13.01	14.41	0.21	5.16	9.55	2.82	0.71	0.55	98.07	b
47.27	4.52	13.59	14.16	0.24	4.82	9.78	3.12	0.78	0.54	98.80	b
47.40	4.55	15.50	14.82	0.21	4.77	9.28	2.99	0.66	0.47	100.65	b
47.49	4.43	13.76	13.78	0.11	5.19	10.13	2.57	0.71	0.47	98.65	b
47.68	4.43	12.68	13.79	0.26	4.90	9.25	3.27	0.83	0.48	97.57	b
47.95	4.64	12.13	14.05	0.22	4.86	9.47	2.83	0.77	0.57	97.48	b
47.97	4.52	13.78	14.22	0.26	4.49	9.36	3.06	0.72	0.52	98.88	b
67.95	0.34	12.79	3.67	0.18	0.21	1.30	5.05	3.45	0.06	95.01	b
68.62	0.24	12.91	3.49	0.10	0.23	1.28	4.96	3.33	0.02	95.19	b
68.82	0.29	12.91	3.65	0.18	0.18	1.27	5.04	3.43	0.07	95.86	b
69.08	0.26	13.06	3.64	0.26	0.20	1.29	5.42	3.53	0.03	96.77	b
69.27	0.26	13.01	3.71	0.05	0.20	1.25	5.06	3.48	0.05	96.34	b
69.65	0.30	13.24	3.83	0.08	0.19	1.34	5.05	3.37	0.05	97.10	b
69.99	0.31	13.29	3.64	0.16	0.21	1.25	5.38	3.43	0.00	97.65	b
70.52	0.32	13.28	3.87	0.23	0.21	1.22	5.16	3.53	0.05	98.37	b
71.04	0.28	13.48	3.59	0.19	0.18	1.16	5.24	3.68	0.06	98.91	b
71.11	0.30	13.33	3.52	0.13	0.22	1.29	5.24	3.55	0.07	98.75	b
71.43	0.28	13.39	3.85	0.06	0.21	1.27	5.27	3.62	0.07	99.45	b
71.78	0.25	13.57	3.83	0.19	0.22	1.22	5.14	3.59	0.05	99.84	b
Rotmeer_VA											
67.85	0.30	12.91	3.53	0.11	0.19	1.26	4.97	3.33	0.10	94.53	c
67.94	0.23	12.91	3.45	0.23	0.18	1.31	4.87	3.35	0.07	94.54	c
67.95	0.26	12.81	3.65	0.15	0.22	1.36	5.27	3.29	0.02	94.96	c
68.13	0.28	12.97	3.94	0.15	0.21	1.30	5.05	3.33	0.07	95.43	c
68.43	0.21	12.96	3.61	0.24	0.21	1.30	4.95	3.28	0.01	95.19	c
68.44	0.32	12.90	3.48	0.17	0.20	1.23	4.97	3.19	0.05	94.96	c
68.98	0.31	13.15	3.87	0.12	0.22	1.32	4.93	3.47	0.04	96.39	c
69.07	0.30	13.24	3.74	0.12	0.19	1.28	5.18	3.45	0.04	96.61	c
69.12	0.32	12.92	3.80	0.13	0.22	1.40	4.88	3.37	0.05	96.22	c
69.20	0.28	13.36	3.91	0.09	0.20	1.30	4.87	3.37	0.03	96.62	c
69.22	0.26	13.21	3.73	0.16	0.20	1.28	4.94	3.57	0.02	96.61	c
69.24	0.25	13.25	3.78	0.18	0.20	1.26	5.10	3.45	0.00	96.71	c
69.44	0.29	13.16	3.69	0.18	0.20	1.27	5.23	3.49	0.03	96.97	c
69.51	0.26	13.31	3.76	0.12	0.19	1.30	4.88	3.34	0.03	96.70	c
69.63	0.32	13.24	3.85	0.10	0.20	1.33	4.89	3.39	0.06	97.01	c
69.69	0.29	13.35	3.55	0.12	0.19	1.32	5.20	3.57	0.00	97.28	c
69.81	0.27	13.32	3.64	0.00	0.20	1.33	5.22	3.45	0.06	97.30	c
69.90	0.32	13.28	3.83	0.15	0.19	1.24	5.12	3.29	0.06	97.36	c
69.94	0.22	12.81	3.64	0.16	0.08	1.01	5.15	3.53	0.00	96.52	c
69.95	0.25	13.33	4.00	0.11	0.21	1.34	5.23	3.33	0.07	97.83	c
70.22	0.25	13.45	3.64	0.11	0.19	1.29	5.31	3.42	0.05	97.93	c
70.27	0.23	13.34	3.94	0.13	0.23	1.36	5.05	3.50	0.04	98.07	c
70.28	0.30	13.34	3.63	0.19	0.21	1.32	5.21	3.52	0.05	98.05	c
70.36	0.29	13.19	3.86	0.13	0.20	1.33	5.12	3.38	0.02	97.89	c
70.44	0.24	13.32	3.95	0.15	0.19	1.28	5.27	3.45	0.04	98.34	c
70.54	0.27	13.46	3.93	0.09	0.18	1.27	5.34	3.46	0.03	98.57	c
70.55	0.29	13.49	3.70	0.14	0.21	1.33	5.07	3.52	0.04	98.33	c
70.87	0.20	13.75	3.62	0.13	0.20	1.41	5.05	3.55	0.05	98.84	c
70.90	0.28	13.46	3.56	0.04	0.17	1.33	5.26	3.43	0.06	98.49	c
70.93	0.28	13.57	3.82	0.24	0.20	1.31	5.17	3.40	0.07	99.00	c

(*continued on next page*)

Table 1 (*continued*)

SiO_2 wt %	TiO_2 wt %	Al_2O_3 wt %	FeO tot wt %	MnO wt %	MgO wt %	CaO wt %	Na_2O wt %	K_2O wt %	P_2O_5 wt %	Total wt %	S/std File
70.99	0.28	13.50	3.73	0.17	0.19	1.28	5.07	3.59	0.04	98.85	c
71.10	0.25	13.71	3.84	0.04	0.17	1.36	5.28	3.52	0.02	99.29	c
71.21	0.31	13.50	3.68	0.17	0.23	1.43	5.33	3.49	0.08	99.44	c
71.29	0.27	13.72	3.37	0.10	0.19	1.18	5.10	3.51	0.03	98.75	c
72.02	0.29	13.86	3.79	0.09	0.20	1.27	5.20	3.55	0.08	100.35	c
Dimnamyra_DA											
67.84	0.24	13.00	3.86	0.15	0.20	1.22	5.22	3.25	0.07	95.05	d
67.93	0.24	13.04	3.86	0.03	0.25	1.37	5.14	3.26	0.08	95.20	d
68.02	0.27	13.27	3.56	0.04	0.17	1.41	4.86	3.16	0.07	94.83	d
68.28	0.24	13.00	3.69	0.14	0.19	1.31	4.99	3.27	0.05	95.17	d
68.39	0.42	13.53	4.44	0.19	0.36	1.65	5.11	3.18	0.16	97.45	d
68.41	0.27	13.57	3.57	0.13	0.20	1.35	5.19	3.33	0.04	96.06	d
68.44	0.36	13.13	3.86	0.24	0.20	1.38	5.04	3.37	0.08	96.11	d
68.52	0.30	13.20	3.80	0.10	0.20	1.24	5.03	3.35	0.04	95.78	d
68.56	0.30	13.17	3.73	0.23	0.20	1.31	5.00	3.24	0.01	95.75	d
68.63	0.28	13.37	3.70	0.14	0.22	1.33	5.14	3.33	0.07	96.22	d
68.65	0.32	13.16	3.85	0.10	0.22	1.38	5.03	3.41	0.08	96.19	d
68.74	0.22	13.23	3.85	0.10	0.22	1.31	5.09	3.38	0.07	96.21	d
68.97	0.31	13.12	3.69	0.15	0.20	1.24	5.06	3.34	0.07	96.16	d
69.01	0.29	13.17	3.74	0.12	0.23	1.27	5.09	3.36	0.04	96.30	d
69.11	0.30	13.39	3.46	0.25	0.18	1.25	4.97	3.37	0.03	96.31	d
69.33	0.30	13.00	3.56	0.18	0.18	1.32	5.47	3.48	0.10	96.92	d
69.40	0.30	13.25	3.77	0.12	0.21	1.24	5.09	3.39	0.10	96.87	d
69.66	0.31	13.32	3.72	0.14	0.21	1.40	4.97	3.57	0.05	97.35	d
69.71	0.32	13.55	3.83	0.23	0.19	1.35	5.05	3.54	0.07	97.84	d
69.77	0.24	13.27	3.91	0.13	0.22	1.36	5.02	3.40	0.10	97.41	d
69.86	0.26	13.29	3.71	0.17	0.22	1.26	5.15	3.49	0.04	97.45	d
70.07	0.30	13.22	3.59	0.17	0.21	1.37	5.33	3.45	0.09	97.80	d
70.10	0.26	13.45	3.84	0.14	0.20	1.23	5.06	3.34	0.06	97.69	d
70.16	0.26	13.54	3.60	0.04	0.22	1.20	5.30	3.34	0.08	97.75	d
70.21	0.30	13.76	3.89	0.04	0.18	1.28	4.82	3.47	0.03	97.98	d
70.21	0.30	13.46	3.66	0.10	0.20	1.35	5.22	3.49	0.10	98.09	d
70.39	0.35	13.62	3.77	0.19	0.23	1.28	5.46	3.31	0.04	98.64	d
70.45	0.28	13.65	3.95	0.21	0.21	1.29	5.10	3.52	0.05	98.72	d
70.50	0.28	13.35	3.63	0.07	0.18	1.36	5.38	3.51	0.05	98.31	d
70.68	0.28	13.43	3.70	0.12	0.21	1.33	5.15	3.56	0.08	98.54	d
70.71	0.28	13.64	4.09	0.12	0.21	1.37	5.22	3.45	0.05	99.14	d
70.79	0.31	13.64	3.91	0.30	0.22	1.29	5.41	3.47	0.07	99.41	d
70.82	0.26	13.23	3.63	0.13	0.23	1.38	5.27	3.58	0.03	98.57	d
71.25	0.27	13.60	3.91	0.07	0.27	1.35	5.17	3.48	0.08	99.45	d
68.75	0.33	13.20	3.84	0.10	0.22	1.29	5.41	3.39	0.05	96.56	e
68.99	0.28	13.04	3.72	0.07	0.18	1.30	5.14	3.48	0.03	96.22	e
69.20	0.31	13.35	3.77	0.19	0.21	1.24	5.16	3.44	0.04	96.92	e
69.56	0.24	13.34	3.92	0.04	0.18	1.27	5.17	3.52	0.03	97.28	e
69.98	0.25	13.30	3.77	0.14	0.21	1.29	5.14	3.46	0.06	97.60	e
70.27	0.28	13.03	3.66	0.15	0.21	1.31	5.13	3.53	0.03	97.60	e
70.62	0.30	13.59	3.87	0.16	0.25	1.28	5.33	3.56	0.07	99.03	e
70.64	0.28	13.57	3.75	0.15	0.21	1.33	5.06	3.43	0.05	98.47	e

member is an Fe–Ti transitional-alkali basalt, only found in those sites around the North Atlantic (Kråkenes and Ashik), and is characterised by (anhydrous) glass compositions of approximately 46.5–49.4 wt % SiO_2, 4.4–5.7 wt % TiO_2, 13.9–17.4 wt % FeO, 4.8–5.8 wt % MgO, 9.1–10.6 wt% CaO, 2.5–3.4 wt % Na_2O, 0.7–0.8 wt % K_2O, 14–17 ppm Rb, 210–250 ppm Zr and 32–36 ppm Nb. Kråkenes is the only site studied in the present paper to preserve tephra with an intermediate composition, which plots between the two end-members along a straight line on elemental bi-plots (Fig. 3). This intermediate composition is also reported in several sites in the Ålesund area (Mangerud et al., 1984; Kvamme et al., 1989; Fig. 3). As previously described by Davies et al. (2001), the VA in Loch Ashik stands out as having a much larger proportion of the basaltic end-member than is present in any other site (Figs. 2 and 3), however the exact proportions are influenced by taphonomic processes and not representative of the primary fallout (Pyne-O'Donnell, 2011). Taken as a whole, this new dataset probably represents the complete chemical composition of the distally-transported phases of the VA eruption.

Compositional data for the Dimna Ash, the R1 tephra from Thornalley et al. (2011), the AF555 tephra and the Suðuroy tephra are plotted in Fig. 4 against the rhyolitic component of the VA. All of these tephra layers have a unimodal rhyolitic composition, and show complete overlap with the VA on all major elements. Trace element data collected on the Dimna Ash (Figs. 4 and 5) also show consistency with the rhyolitic phase of the VA.

Fig. 4c compares the major element composition of the VA (composite data from this study and western Norway) to glass compositions from the Skógar tephra (Norddahl and Haflidason, 1992) and the Sólheimar Ignimbrite (Lacasse et al., 1995; Tomlinson et al., submitted for publication). Whilst the composition of the Sólheimar ignimbrite appears to overlap only with the rhyolitic and intermediate phases of the VA, the Skógar tephra has a compositional range from K-rich undersaturated rhyolite to Fe–Ti basalt that closely resembles the full compositional range of the VA. Norddahl and Haflidason (1992) published two bulk XRF trace element analyses of silicic glass separates from the Skógar tephra, which show broad agreement with the single grain data generated in this study. However, the presence of even small amounts of contaminating mineral or glass fractions in bulk compositional analyses precludes fair comparison of data generated from bulk and single grain techniques and this data is not discussed further here.

Table 2
LA-ICP-MS results for all Vedde Ash and Dimna Ash samples included in this study. "<LOD" indicates signals below 6σ of the background and this varies slightly between analytical runs due to instrument sensitivity. Associated secondary standard analyses files (S/std file) can be found in Supplementary Information Table 2.

Rb	Sr	Y	Zr	Nb	Ba	La	Ce	Pr	Nd	Sm	Eu	Gd	Dy	Er	Yb	Ta	Th	U	Spot (μm)	S/std File
Kråkenes_VA																				
83	120	83	908	129	703	91	198	23	90	19	4	17	17	9	8	8	12	4	34	a
89	115	81	848	124	681	86	185	21	86	17	3	17	16	8	7	6	11	3	34	a
85	119	83	899	127	699	89	195	23	89	19	4	18	17	9	8	7	12	4	34	a
84	120	80	873	125	691	88	195	22	88	20	4	17	16	9	8	7	11	4	34	a
81	116	79	867	124	685	87	191	22	86	18	4	17	17	9	8	8	12	3	34	a
80	117	78	863	123	664	86	188	22	85	18	4	17	16	9	8	7	11	4	34	a
88	124	85	927	129	714	91	198	23	90	19	4	17	17	9	8	7	11	4	34	a
85	123	82	911	129	709	90	198	23	90	19	4	17	17	9	8	8	12	4	34	a
85	122	83	922	129	710	91	200	23	91	21	4	18	17	9	9	8	12	4	34	a
85	124	86	939	129	714	91	202	23	90	19	4	19	17	9	9	8	12	4	34	a
87	154	85	918	129	723	91	199	23	89	20	4	18	16	9	8	8	11	4	34	a
82	119	84	897	126	661	86	187	21	86	20	4	17	16	9	8	7	11	3	34	a
88	124	83	894	129	693	88	192	22	90	19	4	17	16	9	8	7	11	4	34	a
84	118	82	894	129	685	88	193	22	88	19	4	16	16	9	8	7	12	4	34	a
87	121	83	895	128	683	89	192	22	90	19	4	18	16	9	8	7	11	4	34	a
53	292	61	596	82	464	60	133	16	64	14	4	14	12	6	6	5	7	2	34	a
44	342	52	490	69	397	50	112	14	56	14	3	12	11	5	5	4	6	2	34	a
25	394	40	315	46	251	33	75	9	40	10	3	9	8	4	4	3	3	1	34	a
17	430	34	246	36	190	26	61	8	36	8	3	9	7	3	3	2	2	1	34	a
15	437	33	228	34	182	25	59	8	35	8	3	9	7	4	3	2	2	1	34	a
Loch Ashik_VA																				
68	102	69	749	106	578	74	155	17	72	14	<LOD	15	14	<LOD	<LOD	<LOD	9	<LOD	*25*	b
85	113	85	930	127	690	88	192	22	87	18	<LOD	17	16	9	8	7	11	4	*25*	b
14	400	31	214	32	165	22	53	7	32	8	3	7	7	<LOD	<LOD	<LOD	<LOD	<LOD	*25*	b
15	401	31	209	32	164	23	54	7	33	8	<LOD	8	7	<LOD	<LOD	<LOD	<LOD	<LOD	*25*	b
14	407	31	211	32	168	23	54	7	33	8	<LOD	7	7	<LOD	<LOD	<LOD	<LOD	<LOD	*25*	b
14	414	31	214	32	169	23	56	7	33	8	<LOD	8	7	<LOD	<LOD	<LOD	<LOD	<LOD	*25*	b
15	414	32	219	33	170	23	55	7	33	8	<LOD	8	7	<LOD	<LOD	<LOD	<LOD	<LOD	*25*	b
15	416	32	219	33	171	23	57	7	34	8	<LOD	8	7	<LOD	<LOD	<LOD	<LOD	<LOD	*25*	b
14	417	32	222	32	169	24	57	8	34	9	<LOD	9	7	<LOD	<LOD	<LOD	<LOD	<LOD	*25*	b
14	418	32	217	32	169	23	54	7	34	8	<LOD	8	7	<LOD	<LOD	<LOD	<LOD	<LOD	*25*	b
15	420	32	219	33	169	24	56	7	34	8	3	8	7	3	3	2	2	<LOD	*34*	b
16	421	32	222	33	172	23	57	8	35	9	<LOD	8	7	<LOD	<LOD	<LOD	<LOD	<LOD	*25*	b
16	425	31	223	33	176	24	56	7	34	8	<LOD	8	7	<LOD	<LOD	<LOD	<LOD	<LOD	*25*	b
14	426	32	221	33	170	24	56	7	35	8	3	8	7	3	3	2	2	<LOD	*34*	b
15	430	33	226	34	173	24	57	8	36	9	3	8	7	3	3	2	2	<LOD	*34*	b
14	430	32	224	34	177	25	56	7	35	9	<LOD	8	7	4	<LOD	<LOD	<LOD	<LOD	*25*	b
14	432	33	227	34	172	24	57	7	36	9	3	9	7	4	3	2	2	<LOD	*34*	b
14	436	32	232	33	175	24	57	7	33	8	<LOD	8	7	3	<LOD	2	<LOD	<LOD	*25*	b
15	436	33	225	34	176	24	58	7	36	9	3	8	7	3	3	2	2	<LOD	*34*	b
16	441	33	231	34	176	25	59	7	36	8	<LOD	8	7	<LOD	<LOD	<LOD	<LOD	<LOD	*25*	b
Rotmeer_VA																				
78	118	81	848	122	656	84	188	21	83	19	4	16	15	7	7	6	10	<LOD	25	c
73	106	74	750	111	579	71	161	<LOD	70	<LOD	<LOD	<LOD	<LOD	<LOD	<LOD	<LOD	<LOD	<LOD	25	c
79	114	75	809	120	632	81	171	20	82	17	<LOD	15	14	8	<LOD	<LOD	10	<LOD	25	c
78	123	77	782	116	644	80	168	20	83	16	<LOD	<LOD	14	7	<LOD	<LOD	10	<LOD	25	c
86	122	80	829	123	684	81	180	21	83	17	<LOD	16	15	<LOD	<LOD	<LOD	<LOD	<LOD	25	c
79	116	81	845	123	665	87	185	22	90	17	4	16	16	8	8	7	11	4	25	c
79	117	81	864	121	666	88	185	22	90	18	4	16	17	9	8	7	11	3	25	c
Dimnamyra_DA																				
79	120	81	855	126	690	87	180	23	83	18	4	16	15	9	8	7	10	3	*25*	d
78	118	80	849	123	680	88	184	21	85	17	4	16	16	9	7	7	11	4	*25*	d
79	119	79	852	125	663	86	182	22	87	16	3	15	15	8	8	6	10	3	*25*	d
83	121	81	868	122	687	89	194	23	89	19	4	15	16	8	8	7	11	4	*25*	d
73	141	71	775	110	602	79	165	18	73	17	4	16	14	7	7	6	10	3	*25*	d
84	120	82	895	124	679	90	197	22	93	20	4	17	17	9	8	8	12	4	*25*	d
81	103	71	758	113	588	75	168	19	73	17	3	13	12	7	6	5	8	3	*25*	d
77	117	78	864	117	658	84	182	21	86	19	4	17	15	9	8	7	11	3	*25*	d
82	122	84	888	124	693	88	189	22	91	20	4	16	16	9	8	7	12	4	*25*	d
80	120	81	869	128	685	90	186	21	90	18	4	16	16	9	8	7	11	4	*25*	d
79	111	73	794	115	637	81	175	20	79	17	3	16	13	7	7	6	9	3	*25*	d
83	122	83	876	121	706	89	189	22	90	20	4	17	15	8	8	6	11	4	*25*	d

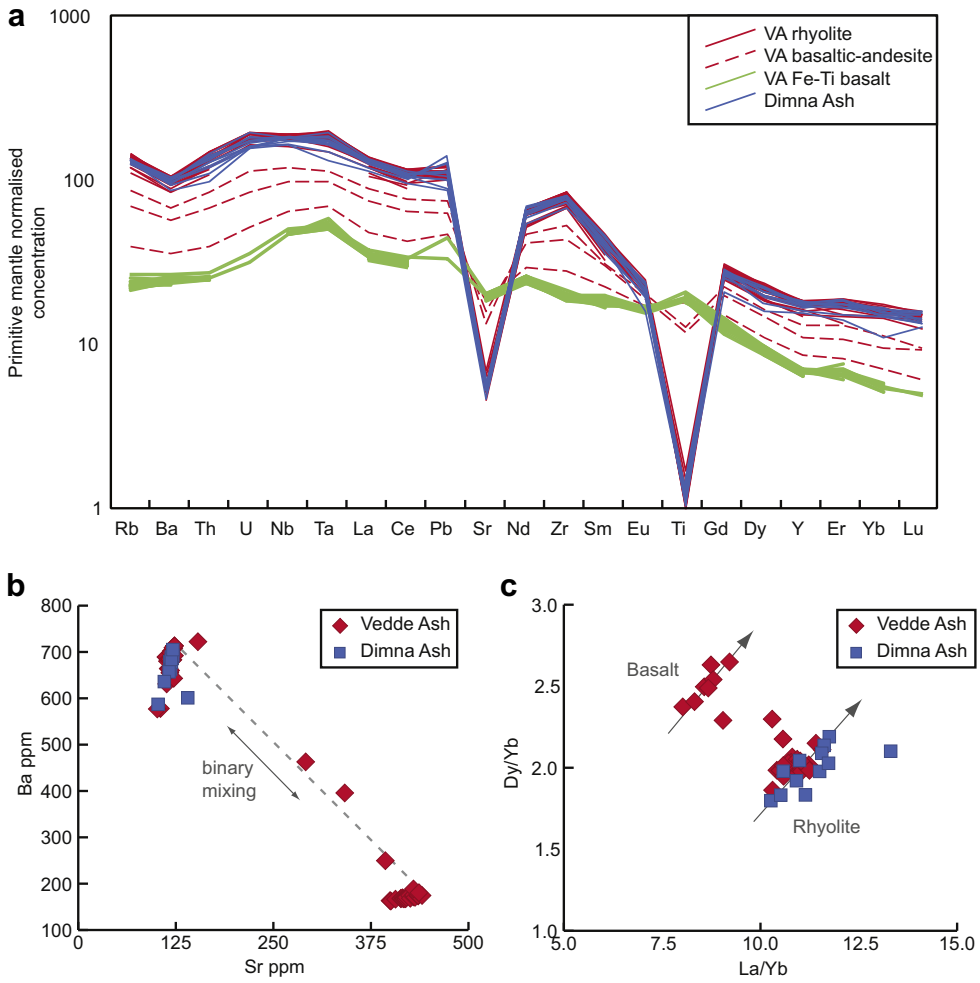

Fig. 5. a) Primitive mantle normalised multi-element diagram showing the glass composition of the Vedde Ash (VA) and the Dimna Ash (Dimna Ash). VA data is combined from Kråkenes, Loch Ashik, and Rotmeer. The trace element composition of the Dimna Ash appears indistinguishable from the rhyolitic fraction of the VA. Primitive mantle normalised values are from Sun and McDonough (1989). (b) Sr vs Ba of VA and Dimna Ash glass shards. The basaltic (Sr enriched) and rhyolite end member compositions are distinct. Intermediate compositions plot along a binary mixing line between the two groups. (c) La/Yb vs Dy/Yb showing the parallel differentiation trends within the end member groups.

4. Discussion

4.1. The petrogenesis of the Vedde Ash

The glass composition of the VA provides some insight into the petrogenesis of the magma.

Intermediate compositions are observed in the VA deposits from Kråkenes (Fig. 3) that plot on a linear array extending between the basaltic and rhyolite end members, suggesting that they are the result of simple binary mixing and hybridisation of two separate melts, and not by fractional crystallisation. Similar mixing processes have been previously postulated for eruptions from Katla system by Lacasse et al. (2007) and Óladóttir et al. (2008).

The small amount of compositional diversity observed in the basaltic and rhyolitic end-member magmas is most likely related to the independent crystallisation of these magma batches. The distinct depletions in Sr, Eu and Ti relative to primitive mantle (Fig. 5) indicate that plagioclase and Fe-Ti oxides were probably the dominant phases crystallising from the rhyolite magma. Smaller Y and Ba anomalies indicate additional fractionation of clinopyroxene and alkali feldspar respectively (Fig. 5). Small degrees of feldspar fractionation within the basalt end-member are indicated by negative Sr and Eu anomalies (Fig. 5). The apparent lack of stratigraphic separation between the basaltic and rhyolitic VA components in the distal environment (Mangerud et al., 1984; Davies et al., 2001; Mortensen et al., 2005) indicates contemporaneous eruption of the two end-member compositions, within days to weeks. Concurrent eruption of basalt and rhyolite is common, with the basalt often triggering the eruption of the rhyolite (e.g., Sparks et al., 1977), however there is insufficient evidence to confirm such a scenario, using the distal glass chemistry alone (see Lacasse et al., 2007; Tomlinson et al., submitted for publication, for a more detailed discussion).

4.2. Dispersal of the Vedde Ash

The wide compositional range of the VA is represented in differing proportions in deposits sampled from across the dispersal area (Fig. 1). This entire range in VA compositions is only observed in the sites in Western Norway (Fig. 3). The deposition of the basaltic phase reaches only the North Atlantic rim, being found only as far as Western Norway, Scotland and Greenland. The basaltic component may remain undetected in some of the northern European sites (see section 1.2), however its absence has been confirmed by thorough investigation of all sediment density fractions at least at a number of the more southerly sites on the

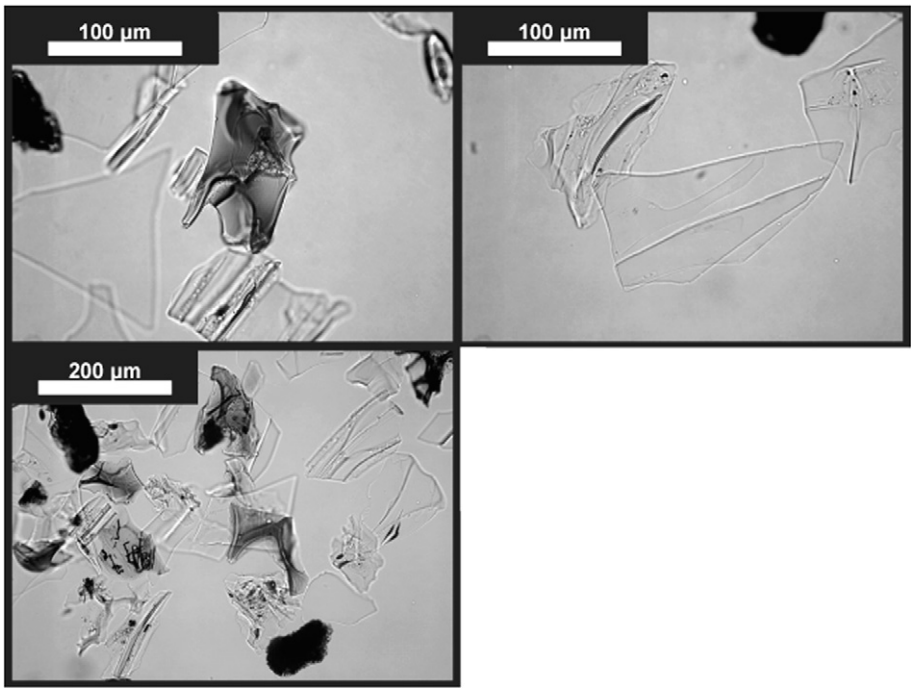

Fig. 6. Photomicrograph of glass shards from the Vedde Ash in Kråkenes, Norway. Light coloured, platy shards are rhyolitic and the darker shards are basaltic to basaltic-andesitic.

European mainland (e.g. Davies et al., 2005; Blockley et al., 2007; Lane et al., 2011b, in press-a, in press-b). The limited dispersal of the basaltic phase is likely to be a result of preferential fallout of the dense basaltic glass limiting the transport distance. The intermediate fraction has not yet been reported outside of Norway. Selective directional dispersal may indicate that this minor compositional phase was only erupted briefly, whilst the column was reduced in height and thus transport was controlled by directional tropospheric, rather than stratospheric winds. The rhyolitic fraction is ubiquitous and reaches all sites, which suggests that this fraction was produced in the highest quantities and was likely transported by both tropospheric and stratospheric winds. The lighter rhyolitic shards are also thin and plate-like (Fig. 6), and therefore are able to be transported further than the denser, blocky, basaltic glass shards (Fisher and Schmincke, 1984).

4.3. Is the Vedde Ash one of a kind?

The value of the VA as a widespread isochronous marker depends upon the secure correlation of distally described deposits back to the type site example from Norway. The rhyolite phase of the Vedde ash is the most widely dispersed phase of the eruption, thus the only phase present at many sites (e.g. Rotmeer, southern Germany). Unfortunately, our results show that the major element glass composition of the rhyolitic phase of the VA is indistinguishable (within errors) from at least four separately described Late Quaternary tephra layers: the Suðuroy Tephra (Wastegård, 2002), the AF555 tephra (Matthews et al., 2011), the Dimna Ash (Koren et al., 2008), and the R1 tephra shards (Thornalley et al., 2011). Furthermore, trace element analysis does not aid discrimination between the compositions of these tephra layers (Fig. 4).

The eruption of a succession of compositionally identical rhyolitic tephras over a periods of >7 ka indicates that either there was a stable magma system or that similar magmatic processes operated repeatedly below Katla during this time. The VA was not the first of these eruptions, being pre-dated by ~3000 years by the Dimna Ash and the R1 tephra. These two older tephras could have hailed from the same eruption event; however, further stratigraphical or chronological information on their occurrences is required to confirm this.

Basaltic eruptions of Katla are also common (Óladóttir et al., 2008), however the VA represents the only distally detected tephra which contains both the basaltic and rhyolitic phases. Thus any distal tephra deposit identified within the middle of the Younger Dryas chronozone that contains both the rhyolitic and basaltic chemistries identified and characterised here, are likely to be the VA. On this basis, our data supports the correlation of the VA and the Skógar Tephra (Fig. 4) found in North Iceland (Norddahl and Haflidason, 1992). The intermediate basaltic-andesite component has only been found in the VA and its presence in a distal deposit would offer further confirmation. Discriminating the VA using glass chemistry only becomes problematic at distal locations where just the rhyolitic component is found, as this cannot be chemically discriminated from the other tephras discussed in this paper. This is where other chronological and stratigraphic information must aid correlation of the tephra units.

5. Conclusions

This study has presented the definitive composition of the VA, as recorded from a number of sites spanning the currently known depositional area. The major and minor element compositions measured are consistent with those previously published but have been supplemented for the first time by single-grain trace element analysis, which will allow more robust correlation of distal deposits of this important Younger Dryas isochronous marker horizon. Despite having no sampled phenocrysts phases or proximal correlative samples, it is still possible to derive information on the petrogenesis of the magma. Our data show that the VA was generated by mixing of separate rhyolitic and basaltic magma batches, which is in agreement with previous theories of bimodal volcanism from the Katla volcano (Lacasse et al., 2007; Óladóttir et al., 2008).

A number of compositionally similar tephra layers have also been compared to the VA. Major, minor, and trace element analysis suggests that there is no means of separating these tephra layers, using composition alone, from the widely dispersed, rhyolitic fraction of the VA. These eruptions however, are well spaced in time (Fig. 2) and therefore by taking into account associated stratigraphical information, it should be possible to assign an unknown distal tephra deposit to the correct volcanic event. A note of caution is however sounded as to carrying out cryptotephra investigations at sites where the associated stratigraphic and/or temporal information is not sufficient to confirm which chronostratigraphic unit an unknown tephra layer lies within (e.g. Housley et al., in press).

The 12.1 ka VA is the most widely dispersed late Quaternary tephra layer from Iceland, and has been well defined stratigraphically (Mangerud et al., 1984; Lowe, 2001), chronologically (Rasmussen et al., 2006), and now also compositionally. Therefore, despite not having a known proximal correlative, the VA remains an effective and unique event marker layer for Lateglacial palaeoenvironmental records across Europe and the North Atlantic.

Acknowledgements

The Authors would like to thank John Inge Svendsen, Victoria Cullen, Sean Pyne-O'Donnell and John Lowe for assistance and advice on this project. This research was funded by the UK Natural Environment Research Council consortium RESET (RESET (NE/E015670/1) and contributes towards the goals of the INTIMATE project (Cost Action ES0907: http://cost-es0907.geoenvi.org/) and the ICEHUS project, funded by the Research Council of Norway. This is RHOXTOR publication number RHOX/0017.

Appendix. Supplementary data

Supplementary data associated with this article can be found in the online version, at doi:10.1016/j.quascirev.2011.11.011.

References

Bakke, J., Lie, O., Heegaard, E., Dokken, T., Haug, G.H., Birks, H.H., Dulski, P., Nilsen, T., 2009. Rapid oceanic and atmospheric changes during the Younger Dryas cold period. Nature Geoscience 2, 202–205.

Bard, E., Arnold, M., Mangerud, J., Paterne, M., Labeyrie, L., Duprat, J., Mélières, M.A., Sønstegaard, E., Duplessy, J.C., 1994. The North Atlantic atmosphere-sea surface 14C gradient during the Younger Dryas climatic event. Earth and Planetary Science Letters 126, 275–287.

Birks, H.H., Gulliksen, S., Haflidason, H., Mangerud, J., Possnert, G., 1996. New radiocarbon dates for the Vedde Ash and the Saksunarvatn Ash from Western Norway. Quaternary Research 45, 119–127.

Birks, H.H., Battarbee, R.W., Birks, H.J.B., 2000. The development of the aquatic ecosystem at Kråkenes Lake, western Norway, during the late glacial and early Holocene – a synthesis. Journal of Paleolimnology 23, 91–114.

Björck, S., Ingolfsson, O., Haflidason, H., Hallsdottir, M., Anderson, N.J., 1992. Lake Torfadalsvatn: a high resolution record of the North Atlantic ash zone I and last glacial-interglacial environmental changes in Iceland. Boreas 21, 15–22.

Björck, J., Wastegård, S., 1999. Climate oscillations and tephrochronology in eastern middle Sweden during the last glacial-interglacial transition. Journal of Quaternary Science 14, 399–410.

Blockley, S.P.E., Pyne-O'Donnell, S.D.F., Lowe, J.J., Matthews, I.P., Stone, A., Pollard, A.M., Turney, C.S.M., Molyneux, E.G., 2005. A new and less destructive laboratory procedure for the physical separation of distal glass tephra shards from sediments. Quaternary Science Reviews 24, 1952–1960.

Blockley, S.P.E., Lane, C.S., Lotter, A.F., Pollard, A.M., 2007. Evidence for the presence of the Vedde Ash in Central Europe. Quaternary Science Reviews 26, 3030–3036.

Bondevik, S., Birks, H.H., Gulliksen, S., Mangerud, J., 1999. Late Weichselian marine 14C reservoir ages at the western coast of Norway. Quaternary Research 52, 104–114.

Bondevik, S., Mangerud, J., 2002. A calendar age estimate of a very late Younger Dryas ice sheet maximum in western Norway. Quaternary Science Reviews 21, 1661–1676.

Bond, G.C., Mandeville, C., Hoffmann, S., 2001. Were rhyolitic glasses in the vedde ash and in the north Atlantic's ash zone 1 produced by the same volcanic eruption? Quaternary Science Reviews 20, 1189–1199.

Brendryen, J., Haflidason, H., Sejrup, H.P., 2010. Norwegian Sea tephrostratigraphy of marine isotope stages 4 and 5: prospects and problems for tephrochronology in the North Atlantic region. Quaternary Science Reviews 29, 847–864.

Davies, S.M., Turney, C.S.M., Lowe, J.J., 2001. Identification and significance of a visible, basalt-rich Vedde Ash layer in a Late-glacial sequence on the Isle of Skye, Inner Hebrides, Scotland. Journal of Quaternary Science 16, 99–104.

Davies, S.M., Wohlfarth, B., Wastegård, S., Blockley, S.P.E., Possnert, G., 2004. Were there two Borrobol Tephras during the early Late-glacial period: implications for tephrochronology? Quaternary Science Reviews 23, 581–589.

Davies, S.M., Hoek, W.Z., Bohncke, S.J.P., Lowe, J.J., O'Donnell, S.P., Turney, C.S.M., 2005. Detection of Lateglacial distal tephra layers in the Netherlands. Boreas 34, 123–135.

Fægri, K., 1940. Quartärgeologische Untersuchungen im Westlichen Norwegen. II. Zur spätquartären Geschichte Jærens. Bergen Museums Årbok. 1939–1940. p.201.

Fisher, R.V., Schmincke, H.U. (Eds.), 1984. Pyroclastic Rocks. Springer-Verlag.

Haflidason, H., Eiriksson, J., van Krefeld, S., 2000. The tephrochronology of Iceland and the North Atlantic region during the middle and Late Quaternary: a review. Journal of Quaternary Science 15, 3–22.

Housley, R.A., Lane, C.S., Cullen, V.L., Weber, M.-J., Riede, F., Gamble, C.S., Brock, F. Icelandic volcanic ash from the Late-glacial open-air archaeological site of Ahrenshöft LA58 D, north Germany. Journal of Archaeological Science, in press. doi:10.1016/j.jas.2011.11.003.

Ingólfsson, O., Norddahl, H., Schomacker, A., 2009. 4 Deglaciation and Holocene Glacial History of Iceland. Developments in Quaternary Science 13, 51–68.

Jochum, K.P., Nohl, U., Herwig, K., Lammel, E., Stoll, B., Hofmann, A.W., 2005. GeoReM: a new geochemical database for reference materials and isotopic standards. Geostandards and Geoanalytical Research 29, 333–338.

Jochum, K.P., Stoll, B., Herwig, K., Willbold, M., Hofmann, A.W., Amini, M., Aarburg, S., Abouchami, W., Hellebrand, E., Mocek, B., Raczek, I., Stracke, A., Alard, O., Bouman, C., Becker, S., Ducking, M., Bratz, H., Klemd, R., de Bruin, D., Canil, D., Cornell, D., de Hoog, C.J., Dalpe, C., Danyushevsky, L., Eisenhauer, A., Gao, Y.J., Snow, J.E., Goschopf, N., Gunther, D., Latkoczy, C., Guillong, M., Hauri, E.H., Hofer, H.E., Lahaye, Y., Horz, K., Jacob, D.E., Kassemann, S.A., Kent, A.J.R., Ludwig, T., Zack, T., Mason, P.R.D., Meixner, A., Rosner, M., Misawa, K.J., Nash, B.P., Pfander, J., Premo, W.R., Sun, W.D.D., Tiepolo, M., Vannucci, R., Vennemann, T., Wayne, D., Woodhead, J.D., 2006. MPI-DING reference glasses for in situ microanalysis: new reference values for element concentrations and isotope ratios. Geochemistry Geophysics Geosystems 7, Q02008. doi:10.1029/2005GC001060.

Johansen, O.I., Henningsmoen, K.E., Sollid, J.L., 1985. Deglaciation of Tingvollhalvoya and adjacent areas, Nordvestlandet, in light of the vegetation development (in Norwegian). Norsk Geografisk Tidsskrift 39, 155–174.

Knudsen, C.G., 2006. Glacier dynamics and Lateglacial environmental changes - evidences from SW Norway and Iceland. PhD. University of Bergen.

Koren, J.H., Svendsen, J.I., Mangerud, J., Furnes, H., 2008. The Dimna Ash – a 12.8 14C ka-old volcanic ash in Western Norway. Quaternary Science Reviews 27, 85–94.

Krüger, L., Paus, A., Svendsen, J.I., Bjune, A.E., 2011. Lateglacial vegetation and palaeoenvironment in W Norway, with new pollen data from the Sunnmøre region. Boreas 40, 616–635.

Kvamme, T., Mangerud, J., Furnes, H., Ruddiman, W.F., 1989. Geochemistry of Pleistocene ash zones in cores from the North Atlantic. Norsk Geologisk Tidsskrift 69, 251–272.

Lacasse, C., Sigurdsson, H., Johannesson, H., Paterne, M., Carey, S., 1995. Source of Ash Zone 1 in the North Atlantic. Bulletin of Volcanology 57, 18–32.

Lacasse, C., Sigurdsson, H., Carey, S.N., Jóhannesson, H., Thomas, L.E., Rogers, N.W., 2007. Bimodal volcanism at the Katla subglacial caldera, Iceland: insight into the geochemistry and petrogenesis of rhyolitic magmas. Bulletin of Volcanology 69, 373–399.

Lane, C.S., Blockley, S.P.E., Bronk Ramsey, C., Lotter, A.F., 2011a. Tephrochronology and absolute centennial scale synchronisation of European and Greenland records for the last glacial to interglacial transition: a case study of Soppensee and NGRIP. Quaternary International 246, 145–156.

Lane, C.S., Andrič, M., Cullen, V.L., Blockley, S.P.E., 2011b. The occurrence of distal Icelandic and Italian tephra in the Lateglacial of Lake Bled, Slovenia. Quaternary Science Reviews 30, 1013–1018.

Lane, C.S., Blockley, S.P.E., Lotter, A.F., Finsinger, W., Filippi, M.L., Matthews, I.P. A regional tephrostratigraphic framework for central and southern European climate archives during the Last Glacial to Interglacial transition: comparisons north and south of the Alps. Quaternary Science Reviews, doi:10.1016/j.quascirev.2010.10.015, in press-a.

Lane, C.S., de Klerk, P., Cullen, V.L. A tephrochronology for the Lateglacial vegetation record of Endinger Bruch, Vorpommern. Journal of Quaternary Science, doi:10.1002/jqs.1521, in press-b.

Larsen, G., Newton, A.J., Dugmore, A.J., Vilmundardoćttir, E.G., 2001. Geochemistry, dispersal, volumes and chronology of Holocene silicic tephra layers from the Katla volcanic system, Iceland. Journal of Quaternary Science 16, 119–132.

Lohne, Ø.S., 2006. Late Weichselian relative sea-level changes and glacial history in Hordaland, Western Norway. PhD thesis. University of Bergen.

Lohne, Ø.S., Bondevik, S., Mangerud, J., Schrader, H., 2004. Calendar year age estimates of Allerød-Younger Dryas sea-level oscillations at Os, western Norway. Journal of Quaternary Science 19, 443–464.

Lohne, Ø.S., Bondevik, S., Mangerud, J., Svendsen, J.I., 2007. Sea-level fluctuations imply that the Younger Dryas ice-sheet expansion in western Norway commenced during the Allerød. Quaternary Science Reviews 26, 2128–2151.

Lohne, Ø.S., Mangerud, J., Svendsen, J.I. Timing of the Younger Dryas glacial maximum in Western Norway. Journal of Quaternary Science, in press. doi:10.1002/jqs.1516.
Long, D., Morton, A.C., 1987. An ash fall within the Loch Lomond Stadial. Journal of Quaternary Science 2, 97–101.
Lowe, J.J., 2001. Abrupt climatic changes in Europe during the last glacial–interglacial transition: the potential for testing hypotheses on the synchroneity of climatic events using tephrochronology. Global and Planetary Change 30, 73–84.
Lowe, J.J., Rasmussen, S.O., Björck, S., Hoek, W.Z., Steffensen, J.P., Walker, M.J.C., Yu, Z.C., 2008. Synchronisation of palaeoenvironmental events in the North Atlantic region during the Last Termination: a revised protocol recommended by the INTIMATE group. Quaternary Science Reviews 27, 6–17.
Mackie, E.A.V., Davies, S.M., Turney, C.S.M., Dobbyn, K., Lowe, J.J., Hill, P.G., 2002. The use of magnetic separation techniques to detect basaltic microtephra in last glacial–interglacial transition (LGIT; 15-10 ka cal. BP) sediment sequences in Scotland. Scottish Journal of Geology 38, 21–30.
Mangerud, J., Andersen, S.T., Berglund, B.E., Donner, J.J., 1974. Quaternary stratigraphy of Norden, a proposal for terminology and classification. Boreas 3, 109–128.
Mangerud, J., Lie, S.E., Furnes, H., Kristiansen, I.L., Lømo, L., 1984. A Younger Dryas Ash Bed in western Norway, and its possible correlations with tephra in cores from the Norwegian Sea and the North Atlantic. Quaternary Research 21, 85–104.
Mangerud, J., Furnes, H., Jóhansen, J., 1986. A 9000-year-old ash bed on the Faroe islands. Quaternary Research 26, 262–265.
Matthews, I.P., Birks, H.H., Bourne, A.J., Brooks, S.J., Lowe, J.J., Macleod, A., Pyne-O'Donnell, S.D.F., 2011. New age estimates and climatostratigraphic correlations for the Borrobol and Penifiler Tephras: evidence from Abernethy Forest, Scotland. Journal of Quaternary Science 26, 247–252.
Mortensen, A.K., Bigler, M., Gronvold, K., Steffensen, J.P., Johnsen, S.J., 2005. Volcanic ash layers from the last glacial termination in the NGRIP ice core. Journal of Quaternary Science 20, 209–219.
Müller, W., Shelley, M., Miller, P., Broude, S., 2009. Initial performance metrics of a new custom-designed ArF excimer LA-ICP-MS system coupled to a two-volume laser-ablation cell. Journal of Analytical Atomic Spectrometry 24, 209–214.
Norddahl, H., Haflidason, H., 1992. The Skogar Tephra, a Younger Dryas marker in north Iceland. Boreas 21, 23–41.
Óladóttir, B.A., Sigmarsson, O., Larsen, G., Thordarson, T., 2008. Katla volcano, Iceland: Magma composition, dynamics and eruption frequency as recorded by Holocene tephra layers. Bulletin of Volcanology 70, 475–493.
Pilcher, J., Bradley, R.S., Francus, P., Anderson, L., 2005. A Holocene tephra record from the Lofoten Islands, Arctic Norway. Boreas 34, 136–156.
Pyne-O'Donnell, S.D.F., 2007. Three new distal tephras in sediments spanning the Last Glacial–Interglacial Transition in Scotland. Journal of Quaternary Science 22, 559–570.
Pyne-O'Donnell, S., 2011. The taphonomy of Last Glacial–Interglacial Transition (LGIT) distal volcanic ash in small Scottish lakes. Boreas 40, 131–145.
Ranner, P.H., Allen, J.R.M., Huntley, B., 2005. A new early Holocene cryptotephra from northwest Scotland. Journal of Quaternary Science 20, 201–208.
Rasmussen, S.O., Andersen, K.K., Svensson, A.M., Steffensen, J.P., Vinther, B.M., Clausen, H.B., Siggaard-Andersen, M.L., Johnsen, S.J., Larsen, L.B., Dahl-Jensen, D., Bigler, M., Röthlisberger, R., Fischer, H., Goto-Azuma, K., Hansson, M.E., Ruth, U., 2006. A new Greenland ice core chronology for the last glacial termination. Journal of Geophysical Research D: Atmospheres 111.
Reimer, P.J., Baillie, M., Bard, E., Bayliss, A., Beck, J.W., Blackwell, P.G., Bronk Ramsey, C., Buck, C.E., Burr, C.E., Edwards, R.L., Friedrich, M., Grootes, P.M., Guilderson, T.P., Hajdas, I., Heaton, T.J., Hogg, A.G., Hughen, K.A., Kaiser, K.F., Kromer, B., McCormac, F.G., Manning, S.W., Reimer, R.W., Richards, D.A., Southon, J.R., Talamo, S., Turney, C.S.M., van der Plicht, J., Weyhenmeyer, C.E., 2009. INTCAL09 and MARINE09 radiocarbon age calibration curves, 0–50,000 years cal BP. Radiocarbon 51, 1111–1150.
Sejrup, H.P., 1989. Quaternary tephrachronology on the Iceland Plateau, north of Iceland. Journal of Quaternary Science 4, 199–214.
Schoning, K., Klingberg, F., Wastegård, S., 2001. Marine conditions in central Sweden during the early Preboreal as inferred from a stable oxygen isotope gradient. Journal of Quaternary Science 16, 785–794.
Sønstegaard, E., Aa, A.R., Klakegg, O., 1999. Younger Dryas glaciation in the Alfoten area, western Norway; evidence from lake sediments and marginal moraines. Norsk Geologisk Tidsskrift 79, 33–45.
Sparks, R.S.J., Sigurdsson, H., Wilson, L., 1977. Magma mixing: a mechanism for triggering acid explosive eruptions. Nature 267, 315–318.
Sun, S.S., McDonough, W.F., 1989. Chemical and isotopic systematics of oceanic basalts: implications for mantle composition and processes. Magmatism in the Ocean Basins 42, 313–345.
Svendsen, J.I., Mangerud, J., 1990. Sea-level changes and pollen stratigraphy on the outer coast of Sunnmore, western Norway. Norsk Geologisk Tidsskrift 70, 111–134.
Thornalley, D.J.R., McCave, I.N., Elderfield, H., 2011. Tephra in deglacial ocean sediments south of Iceland: Stratigraphy, geochemistry and oceanic reservoir ages. Journal of Quaternary Science 26, 190–198.
Tomlinson, E.L., Thordarson, T., Müller, W., Thirlwall, M., Menzies, M.A., 2010. Microanalysis of tephra by LA-ICP-MS – strategies, advantages and limitations assessed using the Thorsmörk ignimbrite (Southern Iceland). Chemical Geology 279, 73–89.
Tomlinson, E.L., Thordarson, T., Lane, C.S., Manning, C.J., Smith, V.C., Blockley, S.P.E, Müller, M., Menzies, M.A. Petrogeneis of the Sólheimar Ignimbrite (Katla, Iceland) and implications for tephrostratigraphy. Geochimica et Cosmochimica Acta, submitted for publication.
Turney, C.S.M., Harkness, D.D., Lowe, J.J., 1997. The use of microtephra horizons to correlate Late-glacial lake sediment successions in Scotland. Journal of Quaternary Science 12, 525–531.
Turney, C.S.M., 1998. Extraction of rhyolitic component of Vedde microtephra from minerogenic lake sediments. Journal of Paleolimnology 19, 199–206.
Turney, C.S.M., van den Burg, K., Wastegård, S., Davies, S.M., Whitehouse, N.J., Pilcher, J.R., Callaghan, C., 2006. North European last glacial–interglacial transition (LGIT; 15-9 ka) tephrochronology: extended limits and new events. Journal of Quaternary Science 21, 335–345.
Van Vliet-Lanoë, B., Gudmundsson, A., Guillou, H., Duncan, R.A., Genty, D., Ghaleb, B., Gouy, S., Rećcourt, P., Scaillet, S., 2007. Limited glaciation and very early deglaciation in central Iceland. Implications for climate change. Comptes Rendus – Geoscience 339, 1–12.
Vorren, K.D., Elverland, E., Blaauw, M., Ravna, E.K., Jensen, C.A.H., 2009. Vegetation and climate c. 12 300–9000 cal. yr BP at Andøya, NW Norway. Boreas 38, 401–420.
Walter-Simonnet, A.V., Bossuet, G., Develle, A.L., Bećgeot, C., Ruffaldi, P., Magny, M., Adatte, T., Rossy, M., Simonnet, J.P., Boutet, J., Zeiller, R., de Beaulieu, J.L., Vanniere, B., Thivet, M., Millet, L., Regent, B., Wackenheim, C., 2008. Chronicle and distribution of lateglacial tephras in the vosges and Jura mountains, and the Swiss plateau. Quaternaire 19, 117–132.
Wastegård, S, 2002. Early to middle Holocene silicic tephra horizons from the Katla volcanic system, Iceland: new results from the Faroe Islands. Journal of Quaternary Science 17, 723–730.
Wastegård, S., Björck, S., Possnert, G., Wohlfarth, B., 1998. Evidence for the occurrence of Vedde Ash in Sweden: radiocarbon and calendar age estimates. Journal of Quaternary Science 13, 271–274.
Wastegård, S., Wohlfarth, B., Subetto, D.A., Sapelko, T.V., 2000a. Extending the known distribution of the Younger Dryas Vedde Ash into northwestern Russia. Journal of Quaternary Science 15, 581–586.
Wastegård, S., Turney, C.S.M., Lowe, J.J., Roberts, S.J., 2000b. New discoveries of the Vedde Ash in southern Sweden and Scotland. Boreas 29, 72–78.